Original Article

Use of High-Resolution Full-Field Optical Coherence Tomography and Dynamic Cell Imaging for Rapid Intraoperative Diagnosis During Breast Cancer Surgery

Houpu Yang, MD [1]; Shuwei Zhang, MM Candidate[1]; Peng Liu, MB[1]; Lin Cheng, MD[1]; Fuzhong Tong, MD[1]; Hongjun Liu, MB[1]; Siyuan Wang, MD[1]; Miao Liu, MD[1]; Chaobin Wang, MD[1]; Yuan Peng, MD[1]; Fei Xie, MD[1]; Bo Zhou, MM[1]; Yingming Cao, MB[1]; Jiajia Guo, MD[1]; Yuanyuan Zhang, MM[2]; Yingteng Ma, MM[2]; Danhua Shen, MM[2]; Peng Xi, PhD[3]; and Shu Wang, MD [1]

BACKGROUND: Although traditional intraoperative assessments (ie, frozen sections) may lower reoperation rates in patients with breast cancer, time/tissue limitations and accuracy concerns have discouraged their routine clinical use. Full-field optical coherence tomography (FFOCT) and dynamic cell imaging (DCI) are novel optical imaging techniques offering rapid histologic approximations that are unfettered by requisite handling steps. This study was conducted to determine the feasibility and diagnostic utility of FFOCT and DCI in examining breast and lymph node specimens during breast cancer surgery. **METHODS:** FFOCT and DCI were applied to normal and cancerous breast tissue, benign breast lesions, and resected axillary lymph nodes. The tissues were then subjected to conventional processing and staining (hematoxylin-eosin) for purposes of comparison. **RESULTS:** A total of 314 specimens, including 173 breast biopsies (malignant, 132; benign/normal, 41) and 141 resected lymph nodes (tumor-positive, 48; tumor-negative, 93), were obtained from 158 patients during breast surgery for prospective imaging evaluations. In breast cancer diagnosis, the minimum sensitivities (FFOCT, 85.6%; DCI, 88.6%) and specificities of optical imaging (FFOCT, 85.4%; DCI, 95.1%) were high, although they diverged somewhat in nodal assessments (FFOCT sensitivity, 66.7%; FFOCT specificity, 79.6%; DCI sensitivity, 83.3%; DCI specificity, 98.9%). **CONCLUSIONS:** These timely and tissue-sparing optical imaging techniques proved highly accurate in diagnosing breast cancer and nodal metastasis. They compare favorably with routine histologic sections and demonstrate their promise in this setting. ***Cancer* 2020;126:3847-3856**. © *2020 American Cancer Society*.

KEYWORDS: breast neoplasms, dynamic cell imaging, intraoperative assessment, optical coherence tomography, sentinel lymph node biopsy.

INTRODUCTION

Traditional intraoperative diagnosis with a frozen section is not routinely implemented in clinical practice because of the time/tissue required and accuracy concerns.[1,2] However, such confirmation has remained attractive to clinicians hoping to lower reoperation rates.[3-5]

Optical coherence tomography (OCT) is a nondestructive imaging technology using light interference to depict the internal microstructural details of tissues.[6-8] Because the optical properties of cellular nuclei are altered by size and textural changes, tumorous and normal tissues may be distinguished on this basis.[9,10] From an oncologic perspective, simple optical scanning enables rapid histologic approximations without conventional tissue processing, sectioning, and staining. Full-field optical coherence tomography (FFOCT) is a variant of OCT that offers enhanced resolution,[11,12] and dynamic cell imaging (DCI), a novel OCT metric complementary to FFOCT, allows the capture of interferogram videos in which cellular contours are defined and metabolic indices are quantifiable.[13] The dynamics of cellular metabolism are then chronicled for an entirely new approach to tissue assessment.[13]

A number of investigative teams have recently experimented with OCT or FFOCT in various diagnostic capacities aimed at brain tumors, pancreatic cancer, lung cancer, and breast lumpectomy margins, and they have reported satisfactory preliminary results.[14-16] DCI has also shown merit in gauging the cell viability of fresh tissues, such as animal retinal explants.[17] However, the prospect of tumor diagnosis via DCI has yet to be explored.

Herein, we address the feasibility and diagnostic utility of FFOCT and DCI in assessing breast lesions and lymph node specimens during breast cancer surgery.

Corresponding Author: Shu Wang, MD, Breast Center, Peking University People's Hospital, 11 Xizhimen S St, Xicheng District, Beijing 100044, People's Republic of China (shuwang@pkuph.edu.cn).

[1]Breast Center, Peking University People's Hospital, Beijing, People's Republic of China; [2]Department of Pathology, Peking University People's Hospital, Beijing, People's Republic of China; [3]College of Engineering, Peking University, Beijing, People's Republic of China

DOI: 10.1002/cncr.32838, **Received:** January 13, 2020; **Revised:** February 6, 2020; **Accepted:** February 16, 2020, **Published online** July 24, 2020 in Wiley Online Library (wileyonlinelibrary.com)

MATERIALS AND METHODS

Light-CT System

The optical scanner (Light-CT; LLTech, Paris, France) used for FFOCT and DCI[11] houses a Linnik interferometer with incoherent illumination. Its object arm holds the sample to be imaged, and in the other arm, a reference mirror is mounted. The en face acquisition of images by FFOCT and DCI relies on a scanning unit of 1.24 mm × 1.24 mm. In areas selected, one unit after another is scanned for eventual compilation, and this provides a larger field of view. FFOCT requires ~2 seconds per unit, as opposed to ~11 seconds for DCI. The native thickness and device resolution is 1 μm. Such systems are capable of optical slicing beneath tissue surfaces at selected depths.

Sample Acquisition and Imaging Process

The local ethics committee of Peking University People's Hospital approved the study protocol, which was registered at ClinicalTrials.gov (NCT03791853). Only patients with surgically treated breast disease qualified for the study, and all granted informed consent before surgical intervention. Benign and malignant breast tissues were obtained from resected specimens, and 1 or 2 blocks were obtained for each sample. The tissue blocks were then simply trimmed to achieve flat surfaces with the thickness limited to 5 mm and the size limited to 25 mm × 25 mm (typically a 10 mm × 10 mm area). Lymph nodes collected during sentinel lymph node biopsy or axillary clearance were bisected on the long axis to present a smooth, fresh tissue surface. All test samples were immersed in a saline solution immediately or within minutes after excision for optical scanning (FFOCT and DCI) before histopathologic processing.

Technically, optical scanning may involve a series of 200 layers at a slice thickness of 1 μm. However, to approximate histologic counterparts and expedite procedures, we chose to scan single layers at depths of 10 μm. In the course of the optical analysis (via Light-CT), no tissue destruction or contrast agents were involved. Each specimen was marked with ink (12 o'clock) at completion and was pinned to a foam board for the matching of optical images with histologic preparations. The tissues were then subjected to routine processing and paraffin embedding. A schematic of the steps taken is shown in Figure 1.

Tissue Processing and Optical/Histologic Image Matching

Paraffin-embedded tissue samples were subsequently sectioned for hematoxylin-eosin (H & E)–stained slide preparations to match in large part with optical images. The workflow designed for this purpose entailed strict specimen orientation and sectioning. Inked edges of scanned specimens served for orientation, with each sample pinned/blocked en bloc onto a small foam board before formalin fixation. A pathology technician then positioned processed specimens in embedding molds and placed scanned surfaces faceup (as in sample holders). The technicians were trained to trim judiciously when they were preparing slides to minimize tissue exhaustion. In the hands of highly experienced technicians, trimming was limited to ~10 μm, the scanning depth typically adopted for optical image acquisition. Ultimately, both optical and histologic images were manually aligned by experienced physicians for comparison.

Imaging Evaluations

Proprietary software (LLTech) was used to view all FFOCT and DCI studies. Two experienced pathologists (Y.Y.Z. and Y.T.M.) were tasked with establishing imaging correlates of histologic findings in breast tissue and lymph nodes. In the review of FFOCT and DCI scans, the architectural hallmarks of abnormal and normal tissue components (breast and nodal) were identified. Related physiologic and pathologic changes, forming the basis for breast and nodal diagnostic criteria, were amassed largely through observation and feedback. Malignant or suspicious breast samples showed clustering or focal hypo-intensity (with or without irregular margins) by FFOCT, with distortion or abnormal scattering of collagen fibers. Clustered or linearly arranged active cells visible by DCI proliferated atypically. In lymph nodes, FFOCT features included a loss of normal structure (especially at the cortex), capsular disruption, hilar abnormalities or absence, and abnormal scattering of collagen fibers. The clustering of active atypical cells by DCI was suspicious or indicative of metastasis. A scoring system, based on the aforementioned imaging features, was subsequently devised to categorize breast tissue and lymph nodes as follows: 0, benign/normal; 1, probably benign; 2, highly suspicious; and 3, probably malignant.

Two breast surgeons (H.P.Y. and S.W.Z.) who trained for 3 hours in imaging diagnosis (by pathologists) were asked to review and independently assess breast and lymph node samples subjected earlier to FFOCT and DCI. Scores of 2 or 3 were considered positive for malignancy, with 0 and 1 equated with negative outcomes. Histologic assessments of pathologists were referenced as gold standards in determining diagnostic accuracy

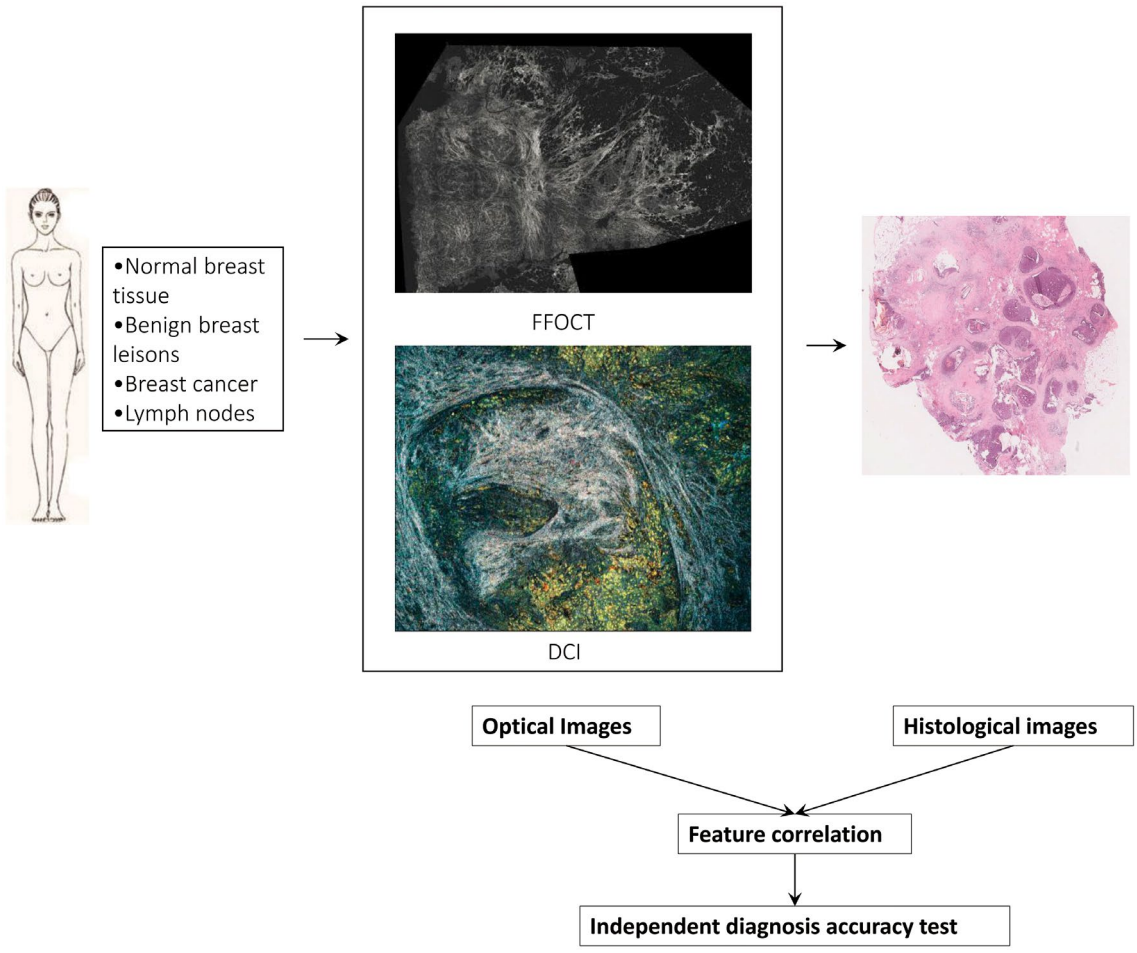

Figure 1. Experimental flow chart. Various tissues acquired during breast surgery were studied by FFOCT and DCI with matched H & E tissue sections for comparison. Diagnostic criteria generated thereby served to assess diagnostic accuracy. DCI indicates dynamic cell imaging; FFOCT, full-field optical coherence tomography.

(ie, sensitivity, specificity, false-negative rate [FNR], and false-positive rate [FPR]). Receiver operating characteristic curve analysis was invoked to compare performances of FFOCT and DCI. To gauge diagnostic agreement between surgeons, Cohen's κ statistic was applied, with values greater than 0.75 indicating excellent agreement, values of 0.4 to 0.75 denoting moderate to good concordance, and values less than 0.4 considered poor.

RESULTS

A total of 314 specimens, including 173 breast biopsies (malignant, 132; benign/normal, 41) and 141 resected lymph nodes (tumor-positive, 48; tumor-negative, 93), were obtained from 158 patients for examination. The average acquisition time was 16 ± 13 minutes. Specimen characteristics are shown in Table 1.

In FFOCT and DCI studies, the normal components of breast tissue (fat, collagen, mammary ducts, and lobules) were easily recognized and corresponded to histologic counterparts (Fig. 2A-C). Normal breast lobules showed moderate signal intensity in FFOCT images and approximated arrangements seen in histologic sections, with a higher backscattering signal of gray-white color by collagen bundles. In DCI mode, normal breast lobular cells were quite visible and formed double layers as expected. Living cells were small, green, and rounded, with collagen fibers appearing white or blue; both were easily distinguished. Similar to the histologic appearance, ductal lumens appeared nearly black by FFOCT amid the hyperscattering of collagenous trabeculae. Ductal cells were also well defined by DCI. Both FFOCT and DCI showed honeycombed

TABLE 1. Characteristics of Analyzed Specimens

Tissue Type/Diagnosis	No. (%)
Breast biopsies imaged	173
Normal tissue	23 (13.3)
Benign lesions	18 (10.4)
Inflammation	2
Atypical hyperplasia	7
Fibroadenoma/benign phyllodes tumor	8
Apocrine adenoma	1
Malignant lesions	132 (76.3)
Invasive ductal carcinoma	92
Invasive lobular carcinoma	11
DCIS	11
LCIS	3
Mucinous carcinoma	5
Others	10
Lymph nodes imaged	141
Tumor present	48 (34)
Isolated cells	0
Micrometastasis	1 (0.7)
Macrometastasis	47 (33.3)
Tumor absent	93 (66.0)

Abbreviations: DCIS, ductal carcinoma in situ; LCIS, lobular carcinoma in situ.

patterns of hyposcattering signal when adipose tissue was scanned.

In pathologic states, tissue landscapes were altered accordingly, with encroachment by in situ (Fig. 2D-F) or invasive breast cancer (Fig. 2G-I) seen as focal or rounded hypo-intensity by FFOCT or as easily distinguished malignant cells (ie, large and bright yellow with dark-staining nuclei) by DCI. It is important to note that the disarray and disappearance of normal structures were the most impressive finding in FFOCT images.

The structural details of lymph nodes (Fig. 3A-C), including membranous capsules, lymphoid follicles, hilar areas, and collagen fibers, were clearly demonstrated by FFOCT and DCI. Normally configured follicles appeared gray in FFOCT images and were marked by a low scattering signal. Signaling in surrounding fibers was similar to that in breast tissue. Numerous closely packed lymphocytes, smaller than breast lobular cells, were discernible by DCI.

In tumor-bearing lymph nodes, lymphoid follicles and other normal components were lacking. Fibrous tangles, tissue disarray, and focal hypo-intensity observed by FFOCT were strongly indicative of metastasis. By DCI, nodal metastases were characterized by the fibrous encircling of malignant cells, as alluded previously (Fig. 3D-F). Other pathologic features, such as microcalcifications, were encountered on occasion.

The potential use of FFOCT or DCI for margin assessment was preliminarily explored in an illustrative patient (Fig. 4). Margin distances determined by FFOCT, DCI, and H & E–stained sections were well matched.

The 2 trained surgeons, having read and scored all FFOCT and DCI studies on the basis of criteria that we devised, were evaluated back to back for diagnostic accuracy. In diagnosing breast malignancies, outcomes were as follows: 91.7% versus 88.6% for sensitivity, 95.1% versus 97.6% for specificity, 8.3% versus 11.4% for FNR, and 4.9% versus 2.4% for FPR by DCI and 88.6% versus 85.6% for sensitivity, 87.8% versus 85.4% for specificity, 11.4% versus 14.4% for FNR, and 12.2% versus 14.6% for FPR by FFOCT. In diagnosing nodal metastases, outcomes were as follows: 91.7% versus 83.3% for sensitivity, 98.9% versus 98.9% for specificity, 8.3% versus 16.7% for FNR, and 1.1% versus 1.1% for FPR by DCI and 81.3% versus 66.7% for sensitivity, 79.6% versus 90.3% for specificity, 18.7% versus 33.3% for FNR, and 20.4% versus 9.7% for FPR by FFOCT. Data on diagnostic accuracy are shown in Table 2. The receiver operating characteristic curves of both surgeons for breast and nodal diagnoses are plotted as Figure 5. The κ values, reflecting diagnostic consistency, were 0.82 (DCI) and 0.90 (FFOCT) for breast specimens and 0.90 (DCI) and 0.62 (FFOCT) for lymph nodes.

DISCUSSION

Breast cancer is the most commonly diagnosed malignancy and the second leading cause of cancer-associated deaths among women.[18] The concept of intraoperative assessment during breast surgery has long been an attractive but controversial option for clinicians.[3-5,19] At present, frozen sections and cytologic imprints require experienced pathologists for hands-on sample preparation and interpretation; this necessitates close interdepartmental cooperation and prolongs operative/anesthesia times. The embedding and trimming entailed may also exhaust or alter precious tissue needed for routine specimen analysis and documentation.[20]

Measures that address this dilemma must meet the following requirements: 1) adequate tissue resolution depicting microstructural details, 2) a high degree of accuracy in distinguishing malignant and benign tissues, 3) noncumbersome technology enabling rapid intraoperative diagnoses, and 4) no tissue waste. A variety of techniques, including conventional ultrasound and radiography, have been investigated as alternatives. The chief disadvantage is that they lack sufficient resolution at a microscopic level.[21] Some emerging optical technologies, such as radiofrequency spectroscopy and Raman spectroscopy, have tentatively qualified as reasonable substitutes[22-26] and shown acceptable sensitivities and specificities. Unfortunately,

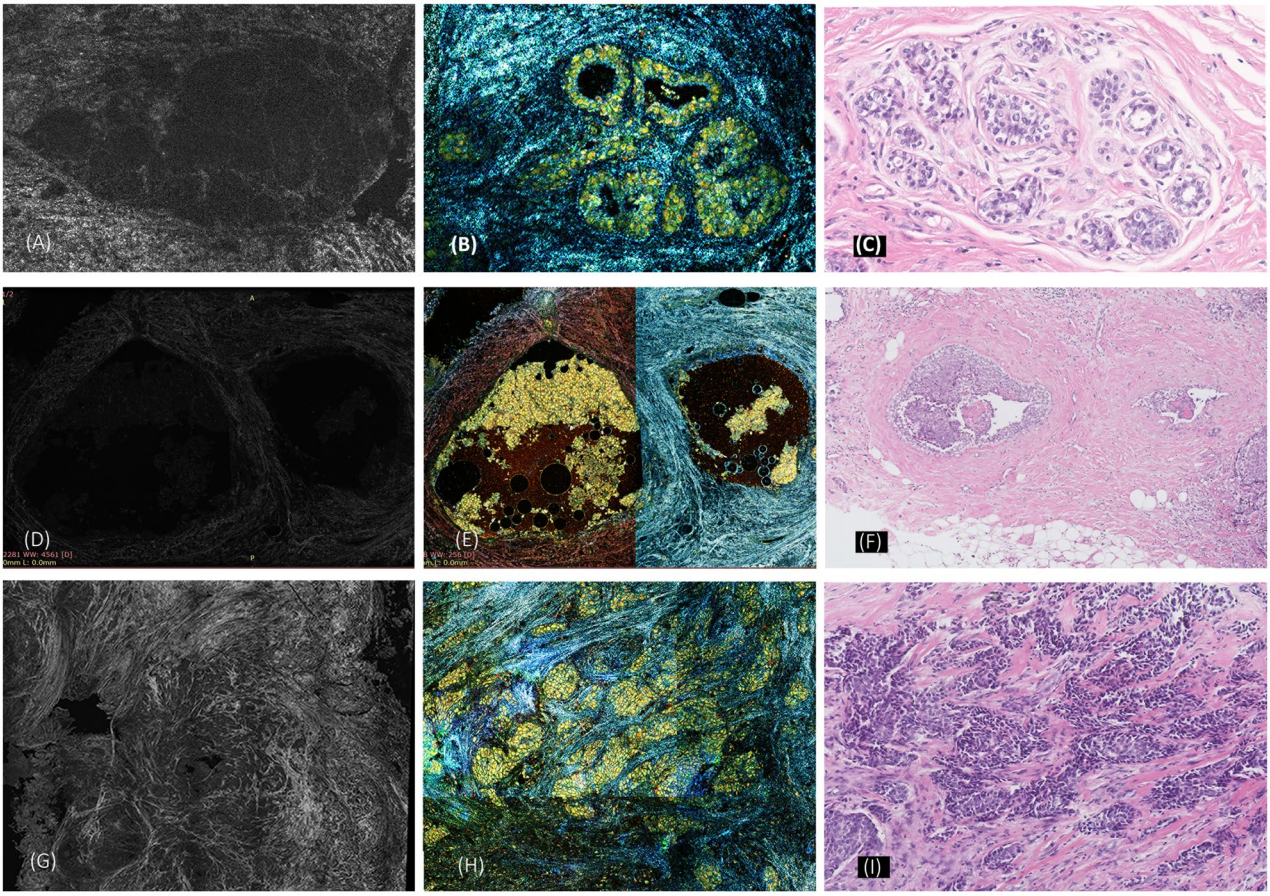

Figure 2. Optical (FFOCT and DCI) and histologic images of normal breast tissue, ductal carcinoma in situ, and infiltrating ductal carcinoma: (A-C) benign breast lobule (note the characteristic chrysanthemum-like, dual-layered cell structure), (D-E) representative views of ductal carcinoma in situ showing intraductal hypo-intensity and clustered bright yellow cells (within the duct) by DCI, and (G-F) typical infiltrating ductal carcinoma visible as local hypo-intensity on FFOCT and nested cells with malignant features (H & E stain). DCI indicates dynamic cell imaging; FFOCT, full-field optical coherence tomography.

inadequate scanning depth and lengthy time requirements have remained problematic.

OCT is a novel and promising nondestructive tissue imaging technology. FFOCT has been used to differentiate benign and malignant breast tissues and provides a platform for diagnostic decision making. Its sensitivity and specificity are roughly 90% and 75%, respectively.[11] In our study, FFOCT performed similarly, and DCI demonstrated superior sensitivity and specificity, with both exceeding 90%. We also examined margins in a representative patient and showed comparable determinations for FFOCT, DCI, and H & E–stained sections, although a larger patient sampling must be tested to confirm these promising results.

Ordinary OCT has been used satisfactorily to detect tumor metastases in lymph nodes (sensitivity, 58.8%; specificity, 81.4%).[27] With its higher resolution, FFOCT was used by Grieve et al[28] to assess 71 axillary lymph nodes in 38 patients, and they achieved high diagnostic accuracy (sensitivity, 92%; specificity, 83%) with the help of pathologists and an imaging expert. In the current study, we introduced DCI to visualize tissues on a cellular scale with metabolic features coupled with the morphologic imaging of FFOCT. This improved both sensitivity and specificity.

Although the time required for FFOCT or DCI approaches that of frozen sections, the steps are certainly not as tedious: No freezing, sectioning, or staining is needed. It is also worth mentioning that the efforts aimed at effective new treatments for patients with breast cancer have increased tissue-based research demands (as in genetic profiling) and created competition for finite quantities of tissue. However, there is no tissue consumed during the rapid acquisition of images by FFOCT or DCI.

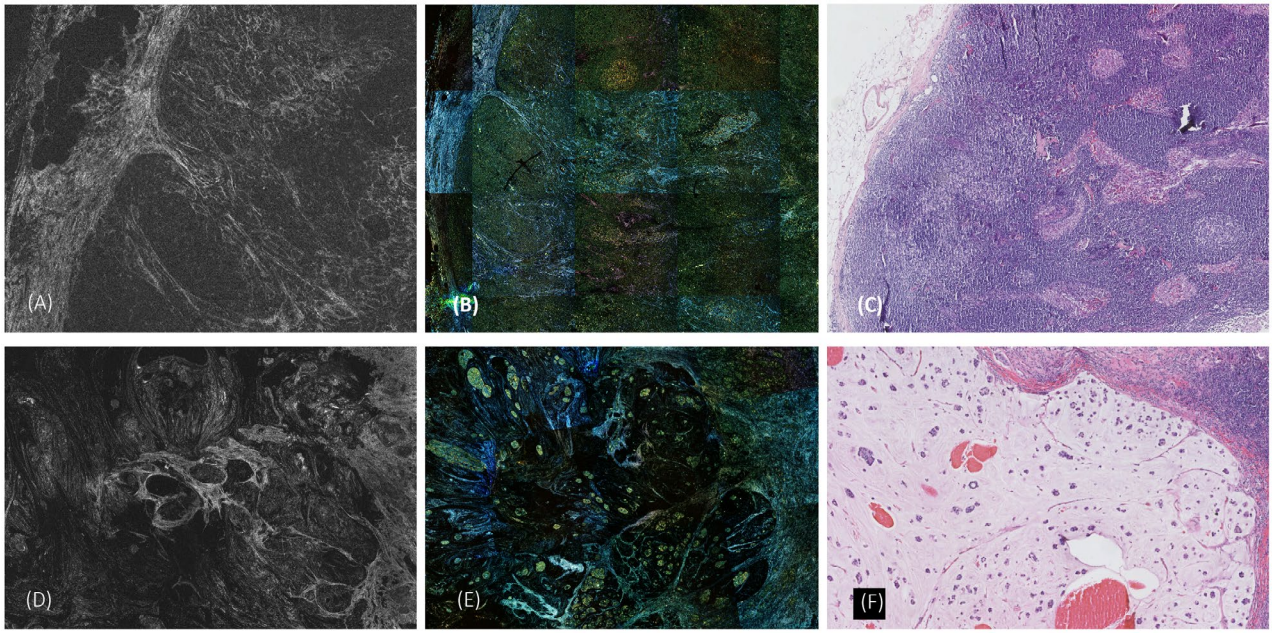

Figure 3. Representative images of tumor-free and tumor-bearing lymph nodes: (A-C) normal nodal structure with a visible capsule, lymphoid follicles, hilum, and collagenous fibers and (D-F) nodal metastasis shown by full-field optical coherence tomography and dynamic cell imaging with cancerous nests similar to those in histologic sections.

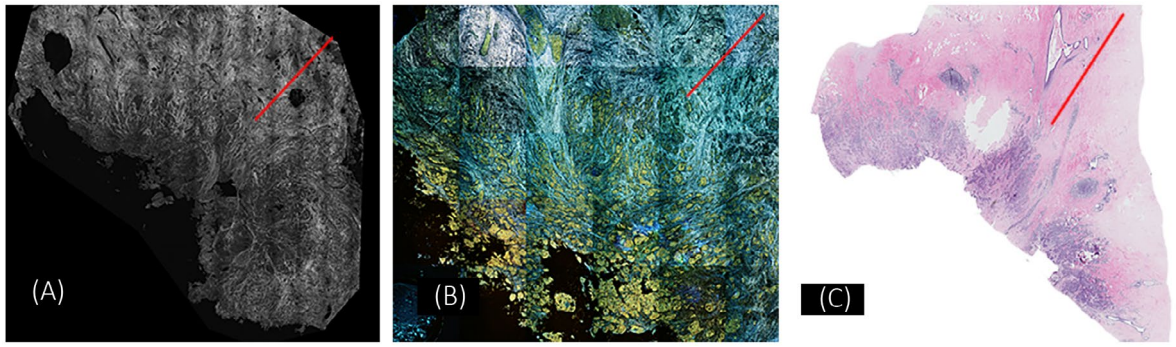

Figure 4. Margin assessment during breast-conserving surgery (illustrative case): the same block assessed with (A) full-field optical coherence tomography, (B) dynamic cell imaging, and (C) histologic sections (H & E stain) with margins of 6.2, 6.8, and 7.6 mm, respectively.

TABLE 2. Diagnostic Accuracy of Surgeons in Assessing Optical Images

Specimen	Investigator	Model	Sensitivity, %	Specificity, %	FNR, %	FPR, %	AUC
Breast	Surgeon 1	DCI	91.7	95.1	8.3	4.9	0.96
		FFOCT	88.6	87.8	11.4	12.2	0.90
	Surgeon 2	DCI	88.6	97.6	11.4	2.4	0.96
		FFOCT	85.6	85.4	14.4	14.6	0.87
Lymph node	Surgeon 1	DCI	91.7	98.9	8.3	1.1	0.98
		FFOCT	81.3	79.6	18.7	20.4	0.84
	Surgeon 2	DCI	83.3	98.9	16.7	1.1	0.93
		FFOCT	66.7	90.3	33.3	9.7	0.82

Abbreviations: AUC, area under the receiver operating characteristic curve; DCI, dynamic cell imaging; FFOCT, full-field optical coherence tomography; FNR, false-negative rate; FPR, false-positive rate.

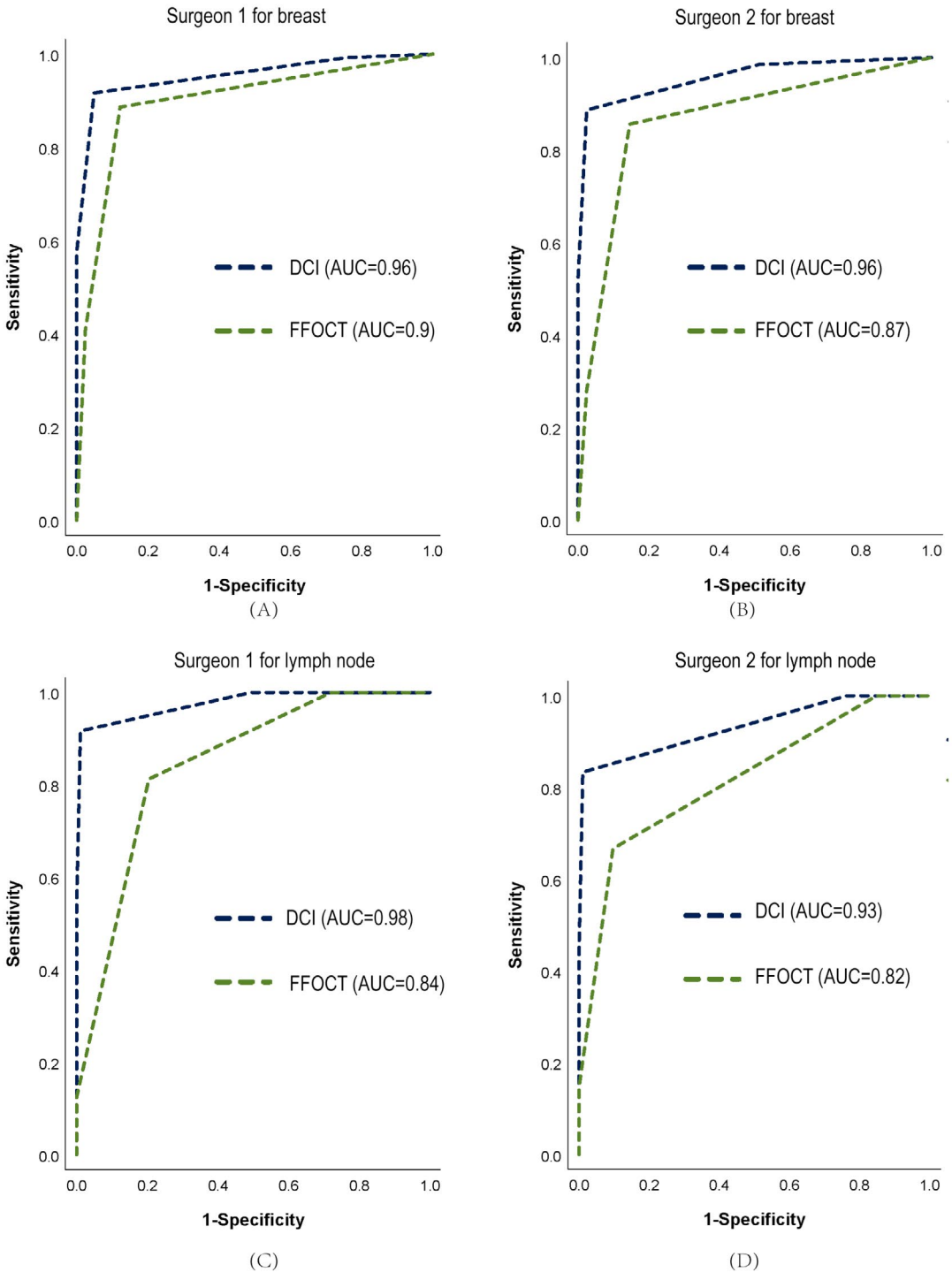

Figure 5. Receiver operating characteristic curves of the performance of surgeons in assessing breast lesions and nodal status. AUC indicates area under the receiver operating characteristic curve; DCI, dynamic cell imaging; FFOCT, full-field optical coherence tomography.

Through this proof-of-concept study, we have demonstrated the diagnostic utility of a combined FFOCT/DCI nonhistologic optical model. Surgeons given short-term training achieved diagnostic accuracy comparable to that achievable with frozen sections.[29] Both the morphology of cells and their arrangement are visible by DCI, and

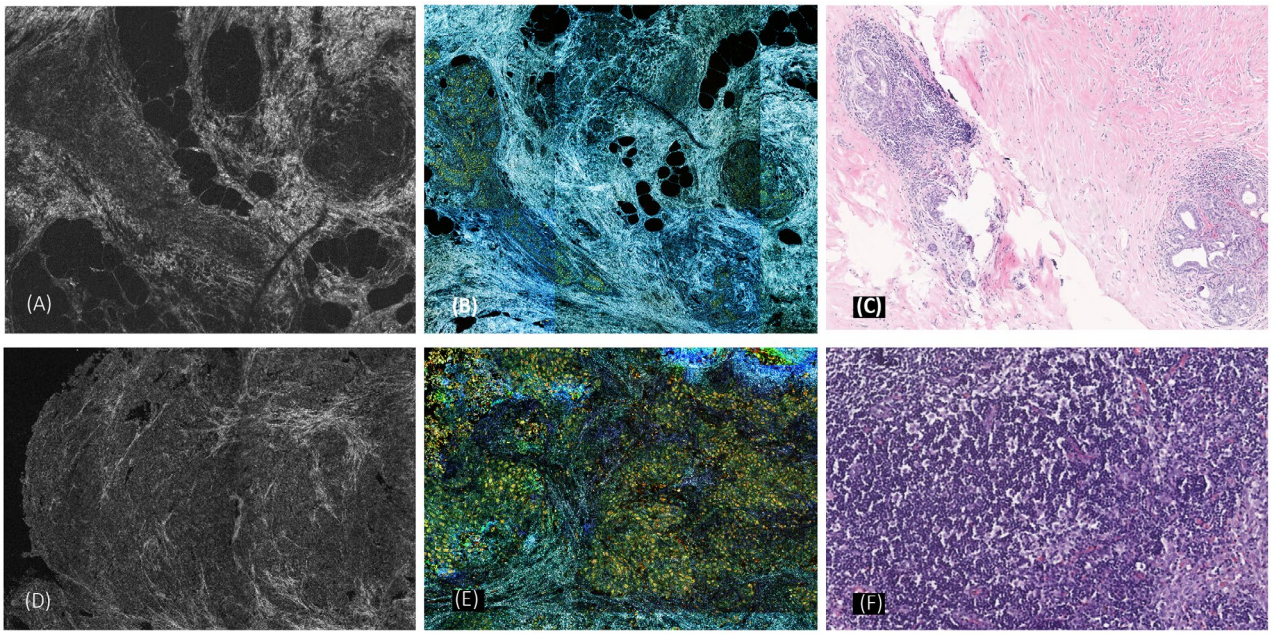

Figure 6. Representative false-positive breast and lymph node diagnoses: (A-C) dense cellularity of a normal lobule mistaken for a proliferative lesion and (D-F) false positivity of a lymph node attributable to DCI-detected clustered active cells, which were not enlarged (an established criterion thereafter).

sometimes nuclei can be seen; this affords close histologic approximations and an appreciable level of consistency. Further interpretative efforts and technologic advances, particularly by way of artificial intelligence, may confer better results.

False diagnoses are the greatest concern in evaluating the merits of a new technique. Herein, in this study, the FNRs of 8.3% and 11.4% for breast tissue as well as 8.3% and 16.7% for lymph nodes were comparable to figures reported for most frozen-section usage in research.[30,31] DCI helped to reduce the FNR under 10%, which was acceptable by intraoperative clinical practice.

False-positive diagnoses should be more carefully weighted because of the consequences of unnecessarily aggressive breast or axillary surgery; ordinary OCT and FFOCT had FPRs of approximately 20%, which was much higher than that for frozen sections, which was reported to be less than 1%. In our study, we achieved FPRs of 1.1% to 4.9% when DCI was used. There were 1 and 2 false-positive cases, respectively, for the 2 surgeons at the early stage of the study. A specimen typifying false positivity of a breast tissue diagnosis is shown in Figure 6A-C. One plausible explanation for such an error may be the difficulty in distinguishing ductal epithelial hyperplasia and carcinoma, which were similar in corresponding histology without further immunohistochemistry testing. The clustering of cells and somewhat heightened metabolism were imaging features common to both but more closely resembling normal breast in cellular details and tissue architecture. With further experience, all other patients with benign hyperplasia were correctly assessed as we categorized such cases as a finding with low suspicion. We also mistook 1 case of an active-appearing lymph node for metastasis (Fig. 6D-F). When taking a closer eye at the clustered active cells, which caused a false diagnosis in this case, we found that the size of the bright "suspicious" cells was much smaller than the size of those in other metastatic nodes and much closer to the size of normal lymph cells. We hypothesized that reactive lymphoid hyperplasia due to prior open biopsy might be the reason for the increase of the cell viability in this special case. The sample size of the current study was not large enough to enable us to define definitive criteria for recognizing the optical characteristics of lymphocytes in special scenarios such as a history of prior surgery, chemotherapy, or comorbid autoimmune disease (eg, systemic lupus erythematosus) in this preliminary study. We hope to optimize the current criteria to avoid false-positive cases in a further, larger cohort.

There were certain limitations to this ex vivo study. First, histologic or cytologic pleomorphism, marked by variability in size, shape, and staining of cells and/or

nuclei, is a critical determinant in the traditional realm of pathology. Such pleomorphism is inherently difficult to recognize during optical imaging. However, pleomorphism depicted through color (hue) and saturation of cells reflecting metabolic status are otherwise captured on DCI and are thought to be useful in differentiating benign and malignant cells and a compensation for the morphologic limitation. Similarly, myoepithelial cells are not easily recognized by optical imaging, and this precludes the separation of in situ and invasive carcinomas, although such a distinction is not required by current guidelines for breast-conserving therapy. Second, the color of cells and their visualization in the DCI model depend on cellular metabolic rates, which are influenced by the time from resection to scanning, neoadjuvant treatment, and tissue type.[13] As a remedy, repeatable comprehensive diagnostic criteria must be formulated and validated in a large-scale clinical trial. Another weakness is the lack of head-to-head comparisons between imaging (FFOCT/DCI) and histologic assessments of surgical margins and sentinel lymph nodes. Because of the less conspicuous nature of malignant cells found beyond the confines of primary growth, it is unclear whether the present level of accuracy is achievable in an actual clinical trial. Optimization of FFOCT/DCI may help to compensate for this shortcoming in the future. Finally, the identification and evaluation of the histologic structure and cell morphology are traditionally considered a specialty of pathologists and require detailed training. This work underscores the rather short learning curve for optical diagnosis and the roles of FFOCT and DCI as adjuncts to traditional pathology. However, the definite learning curves for pathologists and surgeons should be carefully researched in further studies.

Despite some restrictions in this study, we have concluded that diagnosis via optical imaging (ie, FFOCT and DCI) shows high accuracy for breast cancer and demonstrates promising potential for intraoperative diagnosis during breast surgery. Also, we want to emphasize that we have aimed only at introducing a novel intraoperative diagnosis option to aid surgeons with decisions in the theater and that we have not intended to provide a substitute for traditional pathologic diagnosis. The actual value and clinical indications of these new tools should be validated in larger and multicenter trials.

FUNDING SUPPORT

This study was funded by the Clinical Medicine Plus X–Young Scholars Project of Peking University (grants PKU2019LCXQ019 and PKU2018LCXQ004), the Central Universities Fundamental Research Funds, Natural Science Foundation of Beijing Municipality (grant 7202212), and Capital Foundation of Medical Development (grant: A Multi-center Clinical Trial of Intra-operative Artificial Intelligence Aided Evaluation of Sentinel Lymph Nodes Using Dynamic Cellular Imaging Based on Optical Coherence Tomography).

CONFLICT OF INTEREST DISCLOSURES

The authors made no disclosures.

AUTHOR CONTRIBUTIONS

Houpu Yang: Optical tests, formal analysis, software, and writing–review and editing. **Shuwei Zhang:** Optical tests, formal analysis, and writing–original draft. **Peng Liu:** Sample collection and preparation, review of the manuscript. **Lin Cheng:** Sample collection and preparation, review of the manuscript. **Fuzhong Tong:** Sample collection and preparation, review of the manuscript. **Hongjun Liu:** Sample collection and preparation, review of the manuscript. **Siyuan Wang:** Sample collection and preparation, review of the manuscript. **Miao Liu:** Sample collection and preparation, review of the manuscript. **Chaobin Wang:** Sample collection and preparation, review of the manuscript. **Yuan Peng:** Sample collection and preparation, review of the manuscript. **Fei Xie:** Sample collection and preparation, review of the manuscript. **Bo Zhou:** Sample collection and preparation, review of the manuscript. **Yingming Cao:** Sample collection and preparation, review of the manuscript. **Jiajia Guo:** Sample collection and preparation, review of the manuscript. **Yuanyuan Zhang:** Pathology analysis, image correlation, and criteria generation. **Yingteng Ma:** Pathology analysis, image correlation, and criteria generation. **Danhua Shen:** Pathology analysis, image correlation, and criteria generation. **Peng Xi:** Conceptualization and funding acquisition. **Shu Wang:** Conceptualization, funding acquisition, data analysis, and writing–review and editing.

REFERENCES

1. Olson TP, Harter J, Munoz A, Mahvi DM, Breslin T. Frozen section analysis for intraoperative margin assessment during breast-conserving surgery results in low rates of re-excision and local recurrence. *Ann Surg Oncol*. 2007;14:2953-2960.
2. Barakat FH, Sulaiman I, Sughayer MA. Reliability of frozen section in breast sentinel lymph node examination. *Breast Cancer*. 2014;21:576-582.
3. van der Noordaa MEM, Vrancken Peeters N, Rutgers EJT. The intraoperative assessment of sentinel nodes—standards and controversies. *Breast*. 2017;34(suppl 1):S64-S69.
4. Costin AI, Paun I, Varcus F, et al. Intraoperative assessment of sentinel lymph nodes in early-stage breast cancer. *Rom J Morphol Embryol*. 2018;59:1033-1039.
5. Reyna C, DeSnyder SM. Intraoperative margin assessment in breast cancer management. *Surg Oncol Clin N Am*. 2018;27:155-165.
6. Huang D, Swanson EA, Lin CP, et al. Optical coherence tomography. *Science*. 1991;254:1178-1181.
7. Boppart SA, Luo W, Marks DL, Singletary KW. Optical coherence tomography: feasibility for basic research and image-guided surgery of breast cancer. *Breast Cancer Res Treat*. 2004;84:85-97.
8. Carrasco-Zevallos OM, Viehland C, Keller B, et al. Review of intraoperative optical coherence tomography: technology and applications. *Biomed Opt Express*. 2017;8:1607-1637.
9. Wax A, Yang C, Muller MG, et al. In situ detection of neoplastic transformation and chemopreventive effects in rat esophagus epithelium using angle-resolved low-coherence interferometry. *Cancer Res*. 2003;63:3556-3559.
10. Drezek R, Guillaud M, Collier T, et al. Light scattering from cervical cells throughout neoplastic progression: influence of nuclear morphology, DNA content, and chromatin texture. *J Biomed Opt*. 2003;8:7-16.
11. Assayag O, Antoine M, Sigal-Zafrani B, et al. Large field, high resolution full-field optical coherence tomography: a pre-clinical study of human breast tissue and cancer assessment. *Technol Cancer Res Treat*. 2014;13:455-468.
12. Wang J, Xu Y, Boppart SA. Review of optical coherence tomography in oncology. *J Biomed Opt*. 2017;22:1-23.

13. Apelian C, Harms F, Thouvenin O, Boccara AC. Dynamic full field optical coherence tomography: subcellular metabolic contrast revealed in tissues by interferometric signals temporal analysis. *Biomed Opt Express*. 2016;7:1511-1524.
14. Assayag O, Grieve K, Devaux B, et al. Imaging of non-tumorous and tumorous human brain tissues with full-field optical coherence tomography. *Neuroimage Clin*. 2013;2:549-557.
15. van Manen L, Stegehuis PL, Farina-Sarasqueta A, et al. Validation of full-field optical coherence tomography in distinguishing malignant and benign tissue in resected pancreatic cancer specimens. *PLoS One*. 2017;12:e0175862.
16. Jain M, Narula N, Salamoon B, et al. Full-field optical coherence tomography for the analysis of fresh unstained human lobectomy specimens. *J Pathol Inform*. 2013;4:26.
17. Thouvenin O, Boccara C, Fink M, Sahel J, Paques M, Grieve K. Cell motility as contrast agent in retinal explant imaging with full-field optical coherence tomography. *Invest Ophthalmol Vis Sci*. 2017;58:4605-4615.
18. Bray F, Ferlay J, Soerjomataram I, Siegel RL, Torre LA, Jemal A. Global cancer statistics 2018: GLOBOCAN estimates of incidence and mortality worldwide for 36 cancers in 185 countries. *CA Cancer J Clin*. 2018;68:394-424.
19. Lyman GH, Giuliano AE, Somerfield MR, et al. American Society of Clinical Oncology guideline recommendations for sentinel lymph node biopsy in early-stage breast cancer. *J Clin Oncol*. 2005;23:7703-7720.
20. Valdes EK, Boolbol SK, Cohen JM, Feldman SM. Intra-operative touch preparation cytology; does it have a role in re-excision lumpectomy? *Ann Surg Oncol*. 2007;14:1045-1050.
21. St John ER, Al-Khudairi R, Ashrafian H, et al. Diagnostic accuracy of intraoperative techniques for margin assessment in breast cancer surgery: a meta-analysis. *Ann Surg*. 2017;265:300-310.
22. Karni T, Pappo I, Sandbank J, et al. A device for real-time, intraoperative margin assessment in breast-conservation surgery. *Am J Surg*. 2007;194:467-473.
23. Haka AS, Volynskaya Z, Gardecki JA, et al. In vivo margin assessment during partial mastectomy breast surgery using Raman spectroscopy. *Cancer Res*. 2006;66:3317-3322.
24. Butler-Henderson K, Lee AH, Price RI, Waring K. Intraoperative assessment of margins in breast conserving therapy: a systematic review. *Breast*. 2014;23:112-119.
25. Thill M. MarginProbe: intraoperative margin assessment during breast conserving surgery by using radiofrequency spectroscopy. *Expert Rev Med Devices*. 2013;10:301-315.
26. Horsnell JD, Smith JA, Sattlecker M, et al. Raman spectroscopy—a potential new method for the intra-operative assessment of axillary lymph nodes. *Surgeon*. 2012;10:123-127.
27. Nolan RM, Adie SG, Marjanovic M, et al. Intraoperative optical coherence tomography for assessing human lymph nodes for metastatic cancer. *BMC Cancer*. 2016;16:144.
28. Grieve K, Mouslim K, Assayag O, et al. Assessment of sentinel node biopsies with full-field optical coherence tomography. *Technol Cancer Res Treat*. 2016;15:266-274.
29. Houpu Y, Fei X, Yang Y, et al. Use of Memorial Sloan Kettering Cancer Center nomogram to guide intraoperative sentinel lymph node frozen sections in patients with early breast cancer. *J Surg Oncol*. 2019;120:587-592.
30. Cendan JC, Coco D, Copeland EM III. Accuracy of intraoperative frozen-section analysis of breast cancer lumpectomy-bed margins. *J Am Coll Surg*. 2005;201:194-198.
31. Van Diest PJ, Torrenga H, Borgstein PJ, et al. Reliability of intraoperative frozen section and imprint cytological investigation of sentinel lymph nodes in breast cancer. *Histopathology*. 1999;35:14-18.